Visualization of pulmonary vein–left atrium lesions using delayed-enhancement magnetic resonance imaging after cryothermal balloon catheter ablation: A case report

CrossMark

Tsuyoshi Mishima, MD,[*] Koji Miyamoto, MD, PhD,[*] Yoshiaki Morita, MD,[†]
Takashi Noda, MD, PhD,[*] Takeshi Aiba, MD, PhD,[*] Kengo Kusano, MD, PhD[*]

From the [*]Department of Cardiovascular Medicine, National Cerebral and Cardiovascular Center, Suita, Japan, and [†]Department of Radiology, National Cerebral and Cardiovascular Center, Suita, Japan.

Introduction

Electrical pulmonary vein (PV) isolation is an effective technique that is used to treat patients with paroxysmal atrial fibrillation (AF).[1–5] In recent years, PV isolation by cryothermal balloon (CB) ablation has been increasingly adopted by electrophysiology laboratories around the world.[6–8] This technology is associated with more reproducible results and reduced procedural times and may be less influenced by operator dexterity than the traditional point-by-point approach with radiofrequency catheter ablation. Although it may offer the invaluable advantage of achieving PV isolation with a single application, little is known about the extension of the PV–left atrium (LA) lesion after the procedure in clinical practice. Although delayed-enhancement magnetic resonance imaging (DE-MRI) has been reported as a noninvasive tool for visualizing lesions after radiofrequency or CB ablation,[9–13] the relationship between the CB ablation procedure and lesions on DE-MRI results has not yet been assessed in detail.

Case report

A 54-year-old man experiencing palpitations was referred to our hospital, National Cerebral and Cardiovascular Center, for ablation because of drug-refractory paroxysmal AF. After a preprocedural examination including multidetector computed tomography, CB ablation was considered appropriate. After written informed consent was obtained from the patient, the electrophysiological study and ablation were performed under conscious sedation. The standard Brockenbrough technique was used; an 8.5F transseptal sheath (SL0, St. Jude Medical, St. Paul, MN) was introduced into the LA and exchanged for a 12F steerable sheath (FlexCath Advance, Medtronic, Minneapolis, MN). Intravenous heparin was administered to maintain an activated clotting time of >300 seconds immediately after the atrial transseptal puncture.

CB catheter ablation

The 28-mm CB was advanced into the LA via the 12F steerable sheath. The CB was inflated proximal to the left superior PV ostium and then was pushed gently, aiming for complete sealing at the antral aspect of the PV. Contrast medium injected through the central lumen of the CB was used to verify complete occlusion of the PV ostium (Figure 1). A 180-second freeze cycle was then performed for the left superior PV. Although PV potentials could not be recorded for live verification of PV isolation, PV isolation was confirmed after the first freeze cycle. This confirmation was followed by an additional freeze cycle of 180 seconds. A 180-second freeze cycle was applied 2 times for left inferior PV isolation in the same way. Left inferior PV isolation was also confirmed after the first freeze cycle. During cryoenergy application along the right PVs, continuous pacing of the phrenic nerve was performed using a diagnostic catheter (15–25 mm diameter; A-focus, St. Jude Medical) positioned within the superior vena cava. As there have been some difficulty in attaching the balloon to the bottom of the right inferior PV, there remained PV potentials at the bottom of the right inferior PV after a total of 5 freezing times (720 s in all). The right inferior PV was finally isolated 10 seconds after the sixth freeze began, and this isolation was followed by a freeze cycle of 50 seconds. The freeze for right superior PV isolation was performed next. Right superior PV isolation was confirmed after the first freeze cycle of 180

KEY TEACHING POINTS

- Delayed-enhancement magnetic resonance imaging can clearly visualize the lesion set after cryothermal balloon ablation.

- The extent of lesions set and the locations of gaps seem to be associated with the ablation procedure. The gaps were located around right-sided pulmonary veins, to which the cryothermal balloon had difficulty attaching in the ablation procedure.

- The clinical significance of gaps detected by DE-MRI in relation to the recurrence of atrial fibrillation is controversial. Large and prospective studies are required to assess the usefulness of the DE-MRI in clinical practice.

seconds, and an additional 120-second freeze cycle followed. The bidirectional PV-LA conduction block was confirmed by pacing from the coronary sinus and each PV, and all PVs were electrically isolated from the LA after the procedure. The patient was discharged from our hospital 3 days after the procedure, without complications such as thromboemboli, bleeding, or phrenic nerve injury.

Delayed-enhancement magnetic resonance imaging

DE-MRI was performed 1 month after discharge using a 1.5-T scanner (MAGNETOM Sonata, Siemens, Erlangen, Germany) with a 6-channel body array coil. An intravenous bolus of 0.15 mmol/kg gadolinium contrast (Omniscan, Daiichi Sankyo, Tokyo, Japan) was administered 20 minutes before a 3-dimensional (3D) electrocardiographically gated inversion-recovery gradient-echo sequence was applied in the axial orientation. The acquired voxel size was $2.0 \times 1.3 \times 2.5$ mm. Other typical sequence parameters were as follows: repetition time/echo time, 3.5/1.4 milliseconds; flip angle, $10°$; bandwidth, 360 Hz/pixel; inversion time, 300 milliseconds. Scan time for the DE-MRI sequence was approximately 25 seconds during breath hold. Cardiac magnetic resonance images were reconstructed and analyzed using the software module workstation (Ziostation2; Ziosoft, Tokyo, Japan). The scar was extracted by tracing the hyperenhanced area on a source image, and 3D volume-rendering images of the magnetic resonance angiography overlaid with PV-LA scars were reconstructed. The overlaid 3D images were analyzed in terms of whether each PV was completely encircled by the scar and where the suspicious gaps in the lesions were located. Circumferentiality (which was defined as the ratio of the scar to the circumference of each PV) and the volume of the scar around each PV were measured.

DE-MRI could clearly visualize PV-LA lesions around the left and right PVs. (Figures 2 and 3). There was clear, circumferential delayed enhancement around the left superior and inferior PVs, including the carina region. Although there was also clear delayed enhancement around the right superior PV, there were deficits of delayed enhancement at the carina of the right PVs and at the bottom of the right inferior PV. The circumferentialities of the left superior, left inferior, right superior, and right inferior PV were 100%, 100%, 87.1%, and 78.2%, respectively.
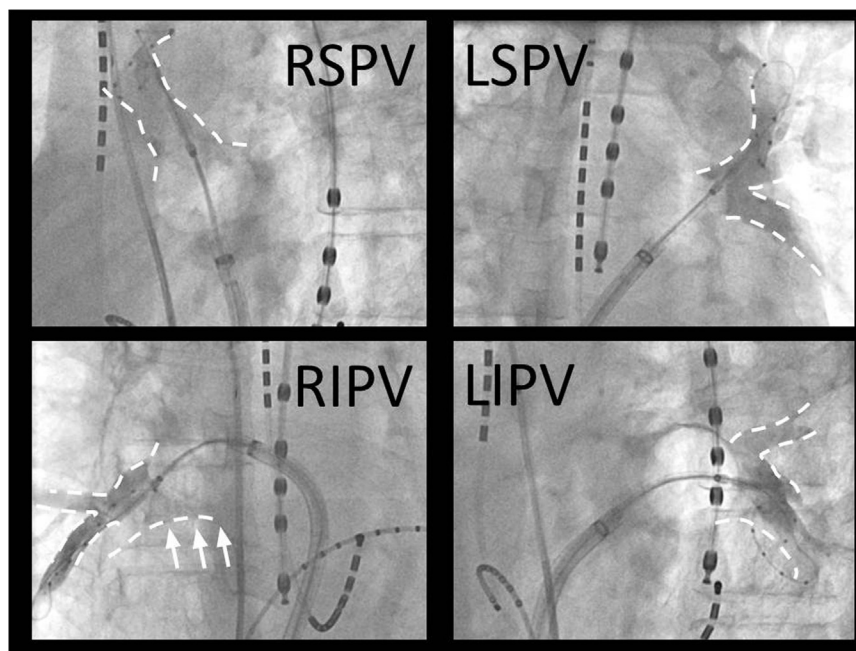

Figure 1 Fluoroscopic images of contrast medium injection at the left superior pulmonary vein (LSPV), left inferior pulmonary vein (LIPV), right superior pulmonary vein (RSPV), and right inferior pulmonary vein (RIPV). LSPV and RSPV are right anterior oblique (RAO) views, and LIPV and RIPV are left anterior oblique (LAO) views, respectively. The broken lines show the pulmonary vein (PV) wall. The arrows in RIPV show the leakage at the bottom of the PV, indicating insufficient cryothermal balloon attachment to the PV ostium.
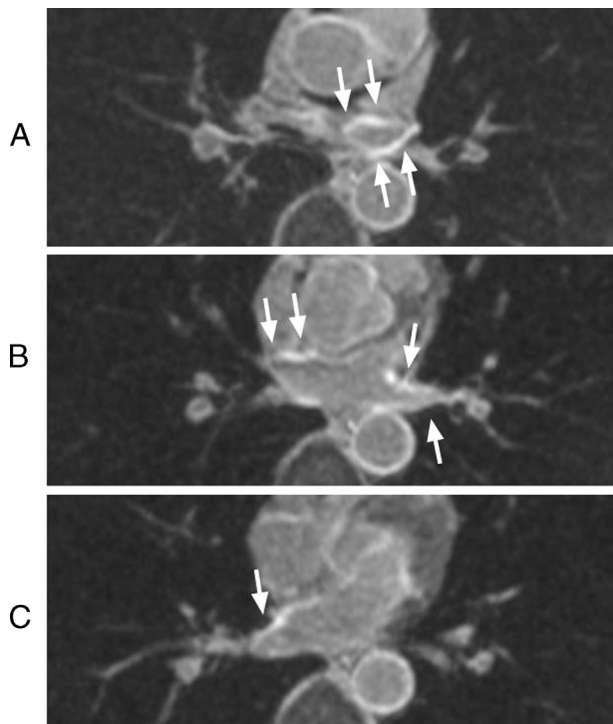
Figure 2 Transaxial images from delayed-enhancement magnetic resonance imaging at the level of **A:** the left superior pulmonary vein (PV), **B:** left inferior and right superior PV, and **C:** right inferior PV. The arrows show the site of delayed enhancement.

Discussion

In this report, we detailed the clearly visualized lesion set after CB ablation by means of DE-MRI. There were homogeneous, completely encircling scars around the left PVs, and there were heterogeneous, incompletely encircling scars around the right PVs. Furthermore, there were suspicious gaps in the lesions at the bottom of the right inferior PV and the right PV carina, areas to which the CB had difficulty attaching in the ablation procedure.

Visualization of the lesions with DE-MRI after AF ablation

There have been previous reports of visualizing the lesions and gaps after radiofrequency ablation for AF with DE-MRI. McGann et al reported both the usefulness of DE-MRI to detect radiofrequency lesions and the correlation between the degree of scarring and procedural outcomes.[9] The researchers concluded that larger LA wall injury might predict less frequent recurrence at short-term follow-up. Segerson et al also reported that the clinical success of PV isolation was better in patients with lesions completely encircling PVs than in patients with incompletely encircling lesions.[10] Bisbal et al reported that DE-MRI accurately identified and localized gaps and reduced the procedural time and radiofrequency application time in repeat ablation sessions.[11] In this case, the lesions were clearly visualized by DE-MRI, which allowed assessment of the scar extension resulting from CB ablation.

Extension of lesions after CB ablation

There have also been reports on the scar extension resulting from CB ablation. Reddy et al evaluated the location of
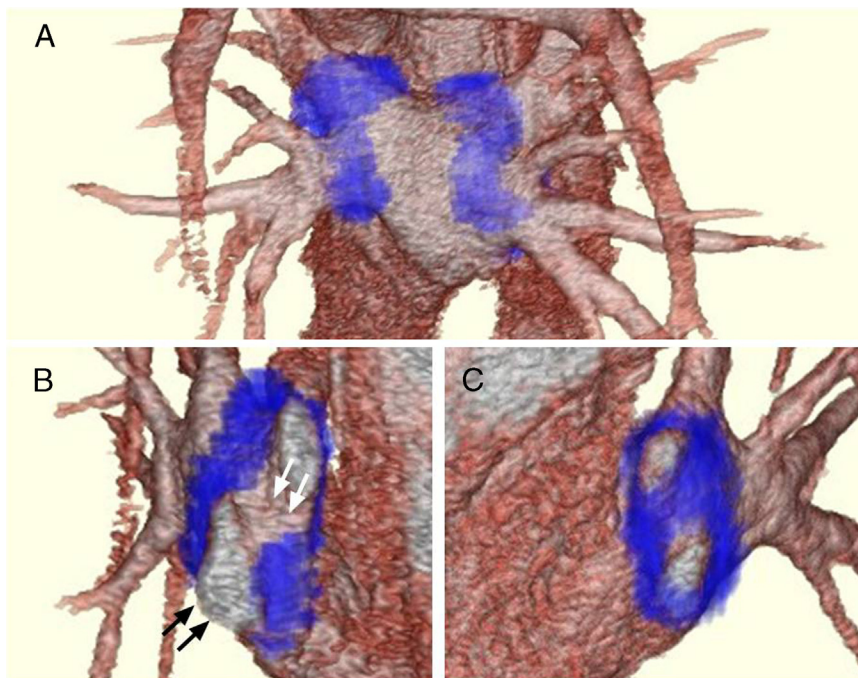

Figure 3 The overlaid images of 3-dimensional reconstructed delayed-enhancement magnetic resonance imaging and magnetic resonance angiogram in **A:** posterior-anterior view, **B:** right lateral view, and **C:** left cranial view. The site of delayed-enhancement is shown as the blue area. Panel A shows the lesion set at the posterior wall of the left atrium, which is wide and antral. Panel B shows the lesion set around the right pulmonary veins (PVs), in which discontinuity of the scar exists at the bottom of the right inferior PV (black arrows) and right PV carina (white arrows). Panel C shows the lesion set around the left PVs, which is dense and completely encircling.

ablation lesions generated by 23-mm first-generation CB catheters using electroanatomic mapping, and they found that the lesion set resided near the PV ostium with little antral penetration.[14] By comparison, Kenigsberg et al reported on a scar extension resulting from 28-mm second-generation CB with electroanatomic mapping, and they found that the lesion set at the LA posterior with the CB catheter was wide and antral.[15] In this case, using second-generation CB, we assessed the lesion set by DE-MRI, which showed wide and dense scarring around PVs, including in the antral area—this finding was in line with those of previous reports.

Suspicious gaps in the lesions

Hunter et al and Halbfass et al have previously shown DE-MRI as a method for assessing the lesion set after CB ablation.[12,13] In these reports, however, the relationship between the DE-MRI findings and the detailed CB ablation procedure was not investigated. In this case report, we assessed the lesion set shown by the DE-MRI in relation to the details of the CB ablation procedure, such as freezing times to isolate each PV. We found that the lesion set was poor at the right inferior PV, where the balloon attachment was difficult and a total of 6 freezing periods were required to electrically isolate the PV.

DE-MRI results showed suspicious gaps in the lesions at the bottom of the right inferior PV and the right PV carina, although the electrical PV isolation was successfully achieved in this case. This inconsistency between DE-MRI and electrophysiological findings may be explained by the loss of transmural lesions. As a result of the difficulty in attaching the balloon to the right inferior PV ostium, it is probable that the cryothermal energy delivery could barely achieve electrical PV isolation and could not achieve the formation of transmural lesions in these regions. Isolation of the right inferior PV with the CB method was reported to require more freezing periods and touch-up ablation because of the technical difficulty with attachment to the PV ostium.[6] Hence, similar to the findings of this case, we found discontinuation of the transmural lesion may exist around electrically isolated PVs. It has been reported that the formation of a transmural lesion is important for successful PV isolation with good clinical outcome.[16,17] However, it is unclear whether the suspicious gap in lesions would affect the outcome of this patient in the chronic phase, because the right inferior PV as AF trigger does not play an important role in AF recurrence.[4,5]

Limitation

There is a possibility that our patient had native scar/fibrosis in the LA before CB balloon. The lack of preablation imaging is a limitation of this report. McGann et al investigated the relationship between the DE-MRI area (structural remodeling) and the volume of the LA.[18] They found that advance structural remodeling (DE-MRI area) was associated with increased LA volume/body surface area. The same group has reported that patients with left ventricular hypertrophy (LVH) had extensive LA structural remodeling as compared with non-LVH patients.[19] They reported that patients with LVH had higher prevalences of hypertension, diabetes, coronary artery disease, and persistent AF compared with those of non-LVH patients. Heart failure has been reported to increase in atrial fibrosis in human and animal models.[20] As for this case, the LA was dilated in neither diameter (28 mm) nor volume index (27 mL/m^2), and the patient had no risk factors for LVH or atrial fibrosis, such as hypertension, diabetes, coronary artery disease, or heart failure. Therefore, we assumed that the lesion set visualized by DE-MRI in this case was ablation-induced scarring but native scar/fibrosis.

Conclusions

This report demonstrated the feasibility of DE-MRI for assessment of the extension of lesions after CB ablation. Although long-term follow-up is required for further discussion, information regarding the extension and gaps of lesions derived from DE-MRI may be useful for treating patients in terms of determining the probability of recurrence and the strategy of the second ablation session.

References

1. Haissaguerre M, Jais P, Shah DC, Garrigue S, Takahashi A, Lavergne T, Hocini M, Peng JT, Roudaut R, Clémenty J. Electrophysiological end point for catheter ablation of atrial fibrillation initiated from multiple pulmonary venous foci. Circulation 2000;101:1409–1417.
2. Oral H, Knight BP, Tada H, Ozaydin M, Chugh A, Hassan S, Scharf C, Lai SW, Greenstein R, Pelosi F Jr, Strickberger SA, Morady F. Pulmonary vein isolation for paroxysmal and persistent atrial fibrillation. Circulation 2002;105:1077–1081.
3. Pappone C, Rosanio S, Augello G, et al. Mortality, morbidity, and quality of life after circumferential pulmonary vein ablation for atrial fibrillation. J Am Coll Cardiol 2003;42:185–197.
4. Haissaguerre M, Jais P, Shah DC, Takahashi A, Hocini M, Quiniou G, Garrigue S, Le Mouroux A, Le Métayer P, Clémenty J. Spontaneous initiation of atrial fibrillation by ectopic beats originating in the pulmonary veins. N Engl J Med 1998:339659–339666.
5. Chen SA, Hsieh MH, Tai CT, Tsai CF, Prakash VS, Yu WC, Hsu TL, Ding YA, Chang MS. Initiation of atrial fibrillation by ectopic beats originating from the pulmonary veins: electrophysiological characteristics, pharmacological responses, and effects of radiofrequency ablation. Circulation 1999;100:1879–1886.
6. Metzner A, Reissmann B, Rausch P, et al. One-year outcome after pulmonary vein isolation using the second-generation 28-mm cryoballoon. Circ Arrhythm Electrophysiol 2014;7:288–292.
7. Mugnai G, Chierchia GB, de Asmundis C, et al. Comparison of pulmonary vein isolation using cryoballoon versus conventional radiofrequency for paroxysmal atrial fibrillation. Am J Cardiol 2014;113:1509–1513.
8. Aytemir K, Gurses KM, Yalcin MU, Kocyigit D, Dural M, Evranos B, Yorgun H, Ates AH, Sahiner ML, Kaya EB, Oto MA. Safety and efficacy outcomes in patients undergoing pulmonary vein isolation with second-generation cryoballoon. Europace 2015;17:379–387.
9. McGann CJ, Kholmovski EG, Oakes RS, et al. New magnetic resonance imaging-based method for detecting the extent of left atrial wall injury after the ablation of atrial fibrillation. J Am Coll Cardiol 2008;52:1263–1271.
10. Segerson NM, Daccarett M, Madger TJ, et al. Magnetic resonance imaging-confirmed ablative debulking of the left atrial posterior wall and septum for treatment of persistent atrial fibrillation: rationale and initial experience. J Cardiovasc Electrophysiol 2010;21:126–132.
11. Bisbal F, Guiu E, Cabanas-Grandio P, et al. CMR-guided approach to localize and ablate gaps in repeat AF ablation procedure. JACC Cardiovasc Imaging 2014;7:653–663.
12. Halbfass PM, Mitlacher M, Turschner O, Brachmann J, Mahnkopf C. Lesion formation after pulmonary vein isolation using the advance cryoballoon and the standard cryoballoon: Lessons learned from late gadolinium enhancement magnetic resonance imaging. Europace 2015;17:566–573.

13. Hunter RJ, Jones DA, Boubertakh R, et al. Diagnostic accuracy of cardiac magnetic resonance imaging in the detection and characterization of left atrial catheter ablation lesions: a multicenter experience. J Cardiovasc Eletrophysiol 2013;24:396–403.

14. Reddy VY, Neuzil P, d'Avila A, Laragy M, Malchano ZJ, Kralovec S, Kim SJ, Ruskin JN. Balloon catheter ablation to treat paroxysmal atrial fibrillation: what is the level of pulmonary venous isolation? Heart Rhythm 2008;5:353–360.

15. Kenigsberg DN, Martin N, Lim HW, Kowalski M, Ellenbogen KA. Quantification of the cryoablation zone demarcated by pre- and post-procedural electro-anatomic mapping in atrial fibrillation patients using the 28-mm second-generation cryoballoon. Heart Rhythm 2015;12:283–290.

16. Wright M, Harks E, Deladi S, Suijver F, Barley M, van Dusschoten A, Fokkenrood S, Zuo F, Sacher F, Hocini M, Haïssaguerre M, Jaïs P. Real-time lesion assessment using a novel combined ultrasound and radiofrequency catheter. Heart Rhythm 2011;8:304–312.

17. Kowalski M, Grimes MM, Perez FJ, Kenigsberg DN, Koneru J, Kasirajan V, Wood MA, Ellenbogen KA. Histopathogenic characterization of chronic radio-frequency ablation lesions for pulmonary vein isolation. J Am Coll Cardiol 2012;59:930–938.

18. McGann C, Akoum N, Patel A, et al. Atrial fibrillation ablation outcome is predicted by left atrial remodeling on MRI. Circ Arrhythm Electrophysiol 2014;7: 23–30.

19. Akkaya M, Higuchi K, Koopmann M, Burgon N, Erdogan E, Damal K, Kholmovski E, McGann C, Marrouche NF. Relationship between left atrial tissue structural remodeling detected using late gadolinium enhancement MRI and left ventricular hypertrophy in patients with atrial fibrillation. Europace 2013;15:1725–1732.

20. Ohtani K, Yutani C, Nagata S, Koretsune Y, Hori M, Kamada T. High prevalence of atrial fibrosis in patients with dilated cardiomyopathy. J Am Coll Cardiol 1995;25:1162–1169.